Navigation System Design using Time-Varying Complementary Filters *

A. Pascoal[†‡] I. Kaminer[‡] P. Oliveira [†]

This paper introduces a new methodology for the design of navigation systems for autonomous vehicles. Using simple kinematic relationships, the problem of estimating the velocity and position of an autonomous vehicle is solved by resorting to special bilinear time-varying filters. These are the natural generalization of linear time-invariant complementary filters that are commonly used to properly merge sensor information available at low frequency with that available in the complementary region. Complementary filters lend themselves to frequency domain interpretations that provide valuable insight into the filtering design process. This paper extends these properties to the time-varying setting by resorting to the theory of linear differential inclusions and by converting the problem of weighted filter performance analysis into that of determining the feasibility of a related set of Linear Matrix Inequalities (LMIs). Using this set-up, the stability of the resulting filters as well as their "frequency-like" performance can be assessed using efficient numerical analysis tools that borrow from convex optimization techniques. The paper introduces the mathematical background that is required for complementary time-varying filter analysis and design and describes its application to the design of a navigation system that estimates position and velocity of an autonomous vehicle by complementing position information available from GPS with the velocity information provided by a Doppler sonar system.

1 Introduction

Currently, there is considerable interest in the development of navigation systems to provide robotic vehicles with the capability to perform complex missions in an autonomous mode. See [1, 4, 15,

*Work supported by the Office of Naval Research under contract N0001497AF00002. The first author was also supported by a NATO Fellowship during his 1996-97 sabbatical leave at the NPS and by MAST-III Program of the EC under contract MAS3-CT97-0092.

† Institute for Systems and Robotics and Department of Electrical Engineering, Instituto Superior Técnico, Av. Rovisco Pais, 1096 Lisboa Codex, Portugal.

‡ Department of Aeronautics and Astronautics, Naval Postgraduate School, Monterey, CA 93943, USA.

16, 18, 21] and the references therein for in depth presentations of navigation systems for aircraft and [8, 13, 22, 24] for an overview of similar systems and related research issues in the underwater robotics area.

Traditionally, navigation system design is done in a stochastic setting using Kalman-Bucy filtering theory [6]. In the case of nonlinear systems, design solutions are usually sought by resorting to Extended Kalman filtering techniques [6]. The stochastic setting requires a complete characterization of process and observation noises, a task that may be difficult, costly, or not suited to the problem at hand. This issue is argued at great length in [7], where the author points out that in a great number of practical applications the filter design process is entirely dominated by constraints that are naturally imposed by the sensor bandwiths. In this case, a design method that explicitly addresses the problem of merging information provided by a given sensor suite over distinct, yet complementary frequency regions is warranted.

Complementary fiters have been developed to addresss this issue explicitly. See for example [7, 18] for a concise introduction to complementary fiters and their applications. In the linear time-invariant setting, filter design is ultimately reduced to the problem of decomposing an identity operator into stable low and high pass transfer functions that operate on complementary sensor information. The bandwith of the low pass tranfer function becomes a tuning parameter aimed at matching the physical characteristics of the "low frequency" sensor. Therefore, the emphasis is shifted from a stochastic to a deterministic framework, where the main objective is to shape the filter closed-transfer functions.

This paper extends complementary filter design and analysis techniques to a time-varying setting, and offers a solution to the problem of estimating the linear position and velocity of a vehicle using time-varying complementary filters. The time-dependence is imposed by the fact that some of the sensors provide measurements in inertial coordinates, while other measurements are naturally expressed in body axis. To merge the information from both types of sensors - while being able to compensate for sensor biases - requires that the rotation matrix from inertial to body axis be explicitly included in the navigation filters. The resulting filters are bilinear and time-varying, but the time dependence is well structured. By exploiting this structure, the problem of filter design and analysis can be converted into that of determining the feasibility of a set of Linear Matrix Inequalities (LMIs) [3, 20] that arise in the theory of linear differential inclusions [2, 3]. As a consequence, the stability of the resulting filters as well as their "frequency-like" performance can be assessed using efficient numerical analysis tools that borrow from convex optimization techniques [3, 17].

The paper is organized as follows. Section 2 reviews some basic mathematical background on linear time-varying systems, induced operator norms, and polytopic systems. Section 3 sets

the motivation for the sections that follow : a simple filtering problem is formulated, and its solution in terms of complementary linear time-invariant filters is described. The new concepts of low and high pass filters for linear time-varying systems are also introduced. Section 4 describes the navigation problem addressed in this paper and formulates it mathematically in terms of an equivalent time-varying filter design problem. Section 5 provides the main theoretical tools for linear time-varying filter design and analyis using the theory of linear matrix inequalities. Section 6 describes a practical algorithm for complementary filter design and illustrates the performance of the new filtering structure in simulation. Section 7 discussed extension of the results reported in previous sections to the case of accelerometers. The paper ends with conclusions.

2 Mathematical background

This section summarizes the mathematical formalism that is required for the study of linear systems, both from an internal and an input-output point of view.

2.1 Linear systems. Internal and input-output descriptions.

We denote by $\mathcal{R}$ (respectively $\mathcal{R}_+$ the set of real (respectively positive real) numbers. The symbol $\mathcal{R}^p$ denotes the Euclidean space of p-tuples of real numbers. Let $\mathcal{X}$ be the linear space of function $calf$ mapping $\mathcal{R}_+$ to $\mathcal{R}^p$. For any $\tau \in \mathcal{R}_+$, Π_τ denotes the projection operator defined for every f in $\mathcal{X}$ by $\Pi_\tau f(t) = f(t)$ when $t \leq \tau$, and 0 otherwise. Let $L_2[0,\infty;\mathcal{R}^p]$ denote the Hilbert space of of Lebesgue measurable functions in $\mathcal{X}$, endowed with the usual norm

$$||f||_2^2 := \int_0^\infty ||f(t)||_2^2 dt$$

and define the extended space $L_{2e}[0,\infty;\mathcal{R}^p] := \{f \in \mathcal{X} : \Pi_\tau f \in L_2[0,\infty;\mathcal{R}^p] \text{ for all finite } \tau \text{ in } \mathcal{R}_+\}$. In the sequel we compress the notation $L_{2e}[0,\infty;\mathcal{R}^p]$ and $L_2[0,\infty;\mathcal{R}^p]$ to L_{2e}^p and L_2^p, respectively. This notation wil be further simplified to L_{2e} and L_2 whenever the dimension of p is not relevant.

An input-output system $\mathcal{G}$ is identified with an operator $\mathcal{G} : L_{2e} \to L_{2e}$ and is said to be causal if $\Pi_\tau \mathcal{G} \Pi_\tau = \Pi_\tau \mathcal{G}$ for all t in $\mathcal{R}_+$. A causal system is $(finite - gain) stable$ if the *induced operator norm* $||\mathcal{G}||_i^2$ (abbv. $||\mathcal{G}||$), defined as

$$||\mathcal{G}|| := \sup\{\frac{||\Pi_\tau \mathcal{G} f||_2}{||\Pi_\tau f||_2} : f \in L_{2e}, \Pi_\tau f \neq 0, t \in \mathcal{R}_+\}$$

is finite. We now focus our attention on the concept of internal stability for linear time-varying (LTV) systems. Throughout this paper, we will restrict ourselves to the class of LTV systems $\mathcal{G}$ with finite-dimensional state-space realizations $\Sigma_\mathcal{G} := \{A(t), B(t), C(t), D(t)\}$ of bounded, piece-wise continuous matrix functions of time. Often, we will use the same symbol $\mathcal{G}$ to denote both an

LTV system and its particular realization $\Sigma_{\mathcal{G}}$, as the meaning wil become clear from the context. A realization is said to be *exponentially stable* if the null solution to the linear differential equation $d\mathbf{x}(\mathbf{t})/dt = A(t)\mathbf{x}(\mathbf{t})$ is uniformly asymptotically stable, that is, there exist positive real constants α and β such that $||\Phi(t,\tau)|| \leq \alpha \exp[-\beta(t-\tau)]$ for all $t \geq \tau$, where $\Phi(t,\tau)$ denotes the transition matrix associated with $A(t)$. To simplify the exposition, we will henceforth refer to an exponentially stable system as *internally stable*, while a (finite-gain) stable system will be simply called stable. If $\mathcal{G} : L_{2e} \rightarrow L_{2e}$ has an internally stable realization, then $\mathcal{G}$ defines a stable operator from $L_2 \rightarrow L_2$.

The extension of these definitions to the case where the operator inputs and outputs belong to the space of essentially bounded functions of time is immediate, and can be found in [23]. Throughout the text, $L_\infty[0,\infty;\mathcal{R}^p]$ (abbv. L_∞) denote the space of Lebesgue measurable functions in $\mathcal{X}$, endowed with the norm

$$||f||_\infty := ess \sup_{t \in \mathcal{R}_+} ||f(t)||_2.$$

If an operator $\mathcal{G}$ admits a state space representation $\Sigma_{\mathcal{G}}$ that is internally stable, then $\mathcal{G}$ maps L_∞ to L_∞ and the corresponding induced operator norm

$$||\mathcal{G}||_{\infty,i} := \sup\{\frac{||\mathcal{G}f||_\infty}{||f||_\infty} : f \in L_\infty, t \in \mathcal{R}_+\}$$

is finite.

2.2 Computation of induced operator norms. Polytopic systems.

Let $\mathcal{G}$ be a stable linear time invariant (LTI) system with a minimal realization $\Sigma_{\mathcal{G}} := \{A, B, C, D\}$, and let $G(s) = C(sI - A)^{-1}B + D$ denote the corresponding transfer matrix. Then, the induced operator norm $||\mathcal{G}||$ equals the $\mathcal{H}_\infty$ norm of G, denoted $||G||_\infty$, where

$$||G||_\infty := \sup_{\omega \in \mathcal{R}} \sigma_{max}(G^T(-j\omega)G(j\omega))$$

and $\sigma_{max}(.)$ denotes the naximum singular value of a matrix. Given a positive integer $\gamma > 0$, then $||\mathcal{G}|| < \gamma$ if and only if there exists a positive definite matrix P that satisfies the matrix inequality [3]

$$\begin{bmatrix} A^TP + PA & PB & C^T \\ B^TP & -\gamma^2 I & D^T \\ C & D & -I \end{bmatrix} < 0 \tag{2.1}$$

If $D = 0$, then the inequality degenerates to

$$\begin{bmatrix} A^TP + PA + C^TC & PB \\ B^TP & -\gamma^2 I \end{bmatrix} < 0 \tag{2.2}$$

The above matrix inequalities are linear matrix inequalities (LMIs) in the matrix variable P. Checking for the existence of $P > 0$ is easily done by resorting to widely available numerical algorithms [17]. In this paper, we will also deal with linear time-varying systems with realizations

$$\{A(t), B(t), C(t), D(t)\} \in \Omega := \mathbf{Co}\{\{A_1, B_1, C_1, D_1\}, ..., \{A_L, B_L, C_L, D_L\}\}$$

where

$$\mathbf{Co}S := \{\sum_{i=1}^{L} \lambda_i \mathcal{A}_i | \mathcal{A}_i \in S, \lambda_1 + ... + \lambda_L = 1\}$$

is the convex hull of the set $S := \{\mathcal{A}_1, ..., \mathcal{A}_n\}$. These systems are usually referred to in the literature as *polytopic differential inclusions* [3]. It can be shown that given a polytopic system $\mathcal{G}$, then $||\mathcal{G}|| < \gamma$ if there exists a positive definite matrix P such that

$$\begin{bmatrix} A_i^TP + PA_i & PB_i & C_i^T \\ B_i^TP & -\gamma^2 I & D_i^T \\ C_i & D_i & -I \end{bmatrix} < 0; i = 1, 2, ..., L. \tag{2.3}$$

Again, checking that such a P exists can be done quite efficiently using highly efficient numerical algorithms.

The results above have their natural counterpart for the case of operators that map L_∞ to L_∞. As discussed in [20], the problem of computing the $L_\infty-$ induced norm of an operator can still be cast in the framework of LMI theory. However, the computational procedure is more complex and requires a line search over a real parameter.

3 Complementary filters. Low and high pass time-varying filters.

This section reviews the basic structure of complementary filters and introduces the key definitions of low and high pass filters for linear time-varying systems.

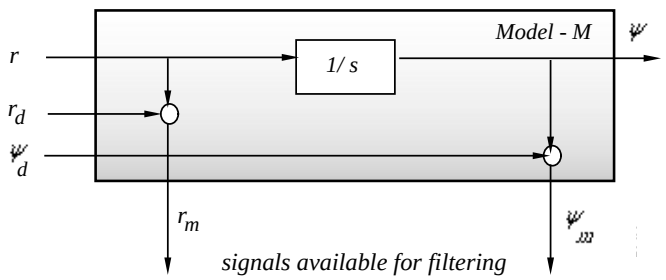

Figure 3.1: Process model.

3.1 Complementary filters: basic concepts and definitions

Complementary filters arise naturally in the context of signal estimation based on measurements provided by sensors over distinct, yet complementary regions of frequency. Brown [7] was the first author to stress the importance of complementary filters in navigation system design. Since then, this subject has been studied in a number of publication that address theoretical as well as practical implementation issues; see for example [1, 16, 18, 19, 21] and the references therein. The key ideas in complementary filtering are very intuitive, and can be simply introduced by referring to the example of Figure 3.1. The figure captures the practical situation where it is required to estimate the heading ψ of a vehicle based on measurements r_m and ψ_m of $r = \dot{\psi}$ and ψ respectively, provided by a rate gyro and a fluxgate compass. The measurements are corrupted by disturbances r_d and ψ_d.

Let $\psi(s)$ and $r(s)$ denote the Laplace Transforms of ψ and r, respectively. Then, for every $k > 0$, $\psi(s)$ admits the stable decomposition

$$\begin{aligned} \psi(s) &= \frac{s+k}{s+k}\,\psi(s) = \frac{k}{s+k}\psi(s) + \frac{s}{s+k}\,\psi(s) \\ &= T_1(s)\psi(s) + T_2(s)\psi(s), \end{aligned} \tag{3.1}$$

where $T_1(s) = k/(s+k)$ and $T_2(s) = s/(s+k)$ satisfy the equality

$$T_1(s) + T_2(s) = I. \tag{3.2}$$

Using the relationship $r(s) = s\psi(s)$, it follows from the above equations that

$$\psi(s) = F_\psi(s)\psi(s) + F_r(s)r(s),$$

where $F_\psi(s) = T_1(s) = k/(s+k)$ and $F_r(s) = 1/(s+k)$. This suggests a filter with the structure

$$\hat{\psi} = \mathcal{F}_\psi \psi_m + \mathcal{F}_r r_m$$

where $\mathcal{F}_\psi$ and $\mathcal{F}_r$ are linear time-invariant operators with transfer functions $F_\psi(s)$ and $F_r(s)$, respectively. Clearly, the filter admits the state space realization

$$\begin{aligned}\dot{\hat{\psi}} &= -k\hat{\psi} + k\psi_m + r_m \\ &= r_m + k(\psi_m - \hat{\psi})\end{aligned} \tag{3.3}$$

that is represented in figure 3.2.

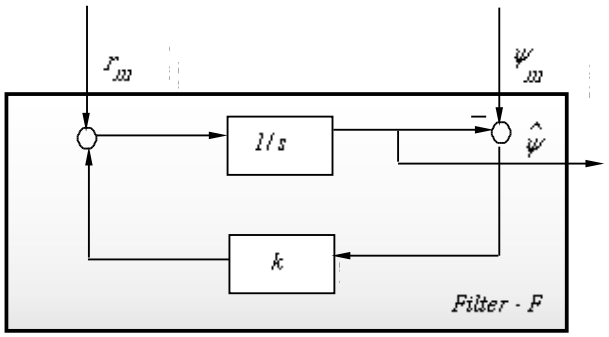

Figure 3.2: Complementary filter.

Let $\mathcal{T}_1$ and $\mathcal{T}_2$ denote linear time-invariant operators with transfer functions $T_1(s)$ and $T_2(s)$, respectively. Simple computations show that

$$\hat{\psi} = (\mathcal{T}_1 + \mathcal{T}_2)\psi + \mathcal{F}_\psi\psi_d + \mathcal{F}_r r_d,$$

that is, the estimate $\hat{\psi}$ consists of an undistorted copy $(\mathcal{T}_1 + \mathcal{T}_2)\psi = \psi$ of the original signal ψ, together with corrupting terms that depend on the measurement disturbances ψ_d and r_d.

Notice the following important properties:

- $T_1(s)$ is low-pass: the filter relies on the information provided by the compass at low frequency only.
- $T_2(s) = I - T_1(s)$: the filter blends the information provided by the compass in the low frequency region with that available from the rate gyro in the complementary region.
- the break frequency is simply determined by the choice of the parameter k.

The frequency decomposition induced by the complementary filter structure holds the key to its practical success, since it mimicks the natural frequency decomposition induced by the physical nature of the sensors themselves: compasses provide reliable information at low frequency only, whereas rate gyros exhibit biases and drift phenomena in the same frequency region and are therefore useful at higher frequencies.

Complementary filter design is then reduced to the computation of the gain k so as to meet a target break frequency that is entirely dictated by the physical characteristics of the sensors. From this point of view, the emphasis is shifted from a stochastic framework - that relies heavily on a correct description of process and measurement noise [7] and the minimization of filter errors - to a deterministic framework that aims at shaping the filter closed-transfer functions.

As convincingly argued in [7], the latter approach is best suited to tackle a large number of practical situations where the characterization of process and measurement disturbances in a stochastic context does not fit the problem at hand, the filter design process being entirely dominated by the constraints imposed by sensor bandwidths. Once this set-up is adopted, however, one is free to use any efficient design method, the design parameters being simply viewed as "tuning knobs" to shape the charateristics of the closed loop operators. In this context, filter design can be done using H_2 or H_∞ design techniques [6, 10, 11, 12, 19]. Filter analysis is easily carried out in the frequency domain using Bode plots. In the simple case described here, the underlying process model can be written as

$$\begin{cases} \dot{\psi} &= r_m - r_d \\ \psi_m &= \psi + \psi_d \end{cases} \tag{3.4}$$

where r_d and ψ_d play the roles of process and measurement disturbances, respectively. Notice the important fact that ψ_m (the measured value of ψ) is an input to the system. In an H_2 setting, the objective is to minimize the estimation error $\psi - \hat{\psi}$ for given values of the covariances of ψ_d and r_d. The optimal solution to this problem has the complementary filter structure described in (3.3). The covariances of ψ_d and r_d are simply viewed as design parameters to vary the break frequency.

In practice, the simple complementary structure described above can be modified to meet additional constraints. For example, to achieve steady state rejection of the rate gyro bias, the filter must be augmented with an integrator to obtain the new complementary filter depicted in figure 3.3 with the realization

$$\begin{aligned} \begin{bmatrix} \dot{x_1} \\ \dot{x_2} \end{bmatrix} &= \begin{bmatrix} -k_1 & 1 \\ -k_2 & 0 \end{bmatrix} \begin{bmatrix} x_1 \\ x_2 \end{bmatrix} + \begin{bmatrix} k_1 \\ k_2 \end{bmatrix} \psi_m + \begin{bmatrix} 1 \\ 0 \end{bmatrix} r_m \\ \hat{\psi} &= \begin{bmatrix} 0 & 1 \end{bmatrix} \begin{bmatrix} x_1 \\ x_2 \end{bmatrix} \end{aligned} \tag{3.5}$$

where x_1 and x_2 denote the states associated with $\hat{\psi}$ and the bias term respectively, and k_1 and k_2 are filter gains. To bring out its relationship with a conventional Kalman filter, the expression

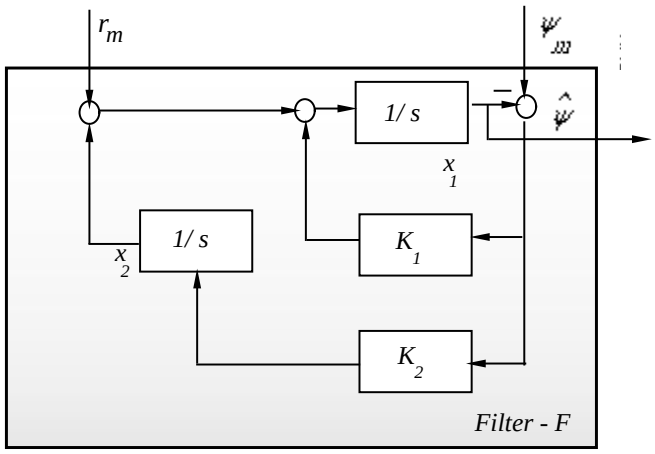

Figure 3.3: Complementary filter with bias estimation.

above can be rewritten as

$$\begin{cases} \dot{\mathbf{x}} &= A\mathbf{x} + Bu + H(y - \hat{y}) \\ \hat{y} &= C\mathbf{x} \end{cases} \tag{3.6}$$

where $\mathbf{x} = [x_1 x_2]^T$, $u = r_m$, $y = \psi_m$, and

$$A = \begin{bmatrix} 0 & 1 \\ 0 & 0 \end{bmatrix}, B = \begin{bmatrix} 1 \\ 0 \end{bmatrix}, C = \begin{bmatrix} 1 & 0 \end{bmatrix}, H = \begin{bmatrix} k_1 \\ k_2 \end{bmatrix}.$$

Simple computations show that in this case

$$\hat{\psi} = (\mathcal{T}_1 + \mathcal{T}_2)\psi + \eta$$

where

$$T_1(s) = \frac{k_1 s + k_2}{s^2 + k_1 s + k_2}, T_2(s) = \frac{s^2}{s^2 + k_1 s + k_2},$$

and $\eta = \mathcal{F}_\psi \psi_d + \mathcal{F}_r r_d$ is a noise term, the intensity of which depends on $F_\psi(s) = T_1(s)$ and $F_r(s) = \frac{s}{s^2 + k_1 s + k_2}$ Again, notice that $T_1(s) + T_2(s) = I$, $T_1(s)$ is low pass, and $T_2(s)$ is high-pass. The filter blends naturally the information provided by the compass at low frequency with that available from the rate gyro in the complementary frequency range, leaving the original signal ψ undistorted. Furthermore, any constant terms in r_d (rate gyro bias) will be naturally rejected at the output since $F_r(0) = 0$. Notice also that the filter rejects naturally high frequency noise present in the fluxgate mesurements.

In view of the discussion above, we henceforth adopt a deterministic framework for complementary filter design and analysis where the objective is to shape the filter transfer functions to obtain desired bandwidths. Furthermore, in preparation for the sections that follow, it is convenient to

formally introduce the definition of a complementary filter for the underlying process model (3.4) (with $r_d = \psi_d = 0$) in a state-space framework, see figure 3.1.

Definition. (r, ψ) **Complementary Filter**. Consider the process model

$$\mathcal{M}_{\psi r} := \begin{cases} \dot{\psi} &= r \\ \psi_m &= \psi \\ r_m &= r \end{cases} \tag{3.7}$$

and a filter $\mathcal{F}$ with realization

$$\begin{aligned} \dot{\mathbf{x}} &= A\mathbf{x} + B_r r_m + B_\psi \psi_m \\ \hat{\psi} &= C\mathbf{x} \end{aligned}$$

Then, $\mathcal{F}$ is said to be a complementary filter for $\mathcal{M}_{\psi r}$ if

- $\mathcal{F}$ it is internally stable
- For every any initial conditions $\psi(0)$ and $\mathbf{x}(0)$ $lim_{t\to\infty}\{\psi(t) - \hat{\psi}(t)\} = 0$.
- $\mathcal{F}$ satisfies a bias rejection property, that is, $lim_{t\to\infty}\hat{\psi} = 0$ when $\psi_m = 0$ and r_m is an arbitrary constant.
- The operator $\mathcal{F}_\psi : \psi_m \to \hat{\psi}$ is a finite bandwith low pass filter.

Clearly, for every $k_1, k_2 > 0$ the filter with realization (3.5) is a complementary filter for the process $\mathcal{M}_{\psi r}$ in (3.7). It is importante to point out that according to the definition above, (3.5) is but one representative of a large class of complementary filters for $\mathcal{M}_{\psi r}$. In this paper, however, and for simplicity of exposition, we restrict ourselves to complementary filter structures similar to (3.5).

3.2 Low and high pass filters: a linear time-varying setting.

The concepts of low pass and high pass filters play a key role in assessing the performance of complemntary filters and are well understood in the case of linear time-invariant systems. We now extend these concepts to the class of linear time-varying systems. The new concepts will play a major role in assessing the performance of the linear time-varying complementary filters that will be introduced later.

Definition. Low pass property. Let $\mathcal{G}$ be a linear, internally stable time-varying system and let $\mathcal{W}_\omega^n$ be a low-pass, linear time-invariant Chebyschev filter of order n and cutoff frequency ω. The system $\mathcal{G}$ is said to satisfy a low pass property with indices (ϵ, n) over $[0, \omega_c]$ if

$$||(\mathcal{G} - I)\, W_{\omega_c}^n|| < \epsilon$$

Definition. Low pass filter with bandwith ω_c. A linear, internally stable time-varying system $\mathcal{G}$ is said to be an (ϵ, n) *low pass filter* with bandwidth ω_c if

- $\lim_{\omega \to 0} ||(\mathcal{G} - I) W_\omega^n||$ is well defined and equals 0.
- $\omega_c := \sup\{\omega : ||(\mathcal{G} - I) W_\omega^n|| < \epsilon\}$, i.e. $\mathcal{G}$ satisfies a low pass property with indices (ϵ, n) over $[0, \omega]$ for all $\omega \in [0, \omega_c)$ but fails to satisy that property whenever $\omega \geq \omega_c$.
- For every $\delta > 0$, there exists $\omega^* = \omega^*(\delta)$ such that $||\mathcal{G}(I - W_\omega^n)|| < \delta$ for $\omega > \omega^*$.

Definition. High Pass Filter with break frequency ω_c. A linear, internally stable time-varying system $\mathcal{G}$ is said to be an (ϵ, n) high pass filter with break frequency ω_c if $(I - \mathcal{G})$ is an (ϵ, n) low pass filter with bandwidth ω_c.

The conditions in the definition of low pass filters generalize the following facts that are obvious in the linear time-invariant case:

- the filter must provide a gain equal to one at zero frequency.
- there is a finite band of frequencies over which the system behaviour replicates very closely that of an identity operator.
- the system gain rolls-off to zero at high frequency.

Notice the role played by the weighting operator $\mathcal{W}_\omega^n$, which was arbitrarily selected as a Chebyschev filter. In practice, the order of the filter can be made sufficiently large so as to make it effectively select the "low frequency components" of the input signal.

4 Navigation system design: problem formulation

This section desribes the navigation problem that is the main focus of the paper and formulates it mathematically in terms of an equivalent filter desig problem. For the sake of clarity, we first introduce some basic notation and summarize the kinematic equations for a general vehicle.

4.1 Notation. Vehicle kinematics: a summary.

Let $\{\mathcal{I}\}$ be a reference frame, and let $\{\mathcal{B}\}$ denote a body-fixed frame that moves with the vehicle. The following notation is required:

- $\mathbf{p} = [x\ y\ z]^T$ - position of the origin of $\{\mathcal{B}\}$ measured in $\{\mathcal{I}\}$.

- ${}^I\mathbf{v} = [\dot{x}\ \dot{y}\ \dot{z}]^T$ - linear velocity of the origin of $\{\mathcal{B}\}$ measured in $\{\mathcal{I}\}$.
- $\mathbf{v} = [u\ v\ w]^T$ - linear velocity of the origin of $\{\mathcal{B}\}$ with respect to $\{\mathcal{I}\}$, resolved in $\{\mathcal{B}\}$
- $\boldsymbol{\omega} = [p\ q\ r]^T$ - angular velocity of $\{\mathcal{B}\}$ with respect to $\{\mathcal{I}\}$, resolved in $\{\mathcal{B}\}$.
- $\boldsymbol{\lambda} = [\phi\ \theta\ \psi]^T$ - vector of roll, pitch, and yaw angles that parametrize locally the orientation of frame $\{\mathcal{B}\}$ with respect to $\{\mathcal{I}\}$.

Given two frames $\{\mathcal{A}\}$ and $\{\mathcal{B}\}$, ${}^A_B\mathcal{R}$ denotes the rotation matrix from $\{\mathcal{B}\}$ to $\{\mathcal{A}\}$. In particular, ${}^I_B\mathcal{R}$ (abbreviated $\mathcal{R}$) is the rotation matrix from $\{\mathcal{B}\}$ to $\{\mathcal{I}\}$, parametrized locally by $\boldsymbol{\lambda}$, that is, $\mathcal{R} = \mathcal{R}(\boldsymbol{\lambda})$. Since $\mathcal{R}$ is a rotation matrix, it satisfies the orthonormality condition $\mathcal{R}^T\mathcal{R} = I$. Given the angular velocity vector $\boldsymbol{\omega}$, then

$$\dot{\boldsymbol{\lambda}} = Q(\boldsymbol{\lambda})\boldsymbol{\omega}$$

where $Q(\boldsymbol{\lambda})$ is a matrix that relates the derivative of $\boldsymbol{\lambda}$ with $\boldsymbol{\omega}$. The following kinematic relations apply [4]:

$$\dot{\mathbf{p}} = {}^I\mathbf{v} = \mathcal{R}\mathbf{v} \text{ and} \tag{4.1}$$

$$\dot{\mathcal{R}} = \mathcal{R}\mathcal{S}(\boldsymbol{\omega}), \tag{4.2}$$

where

$$\mathcal{S}(\boldsymbol{\omega}) := \begin{bmatrix} 0 & -\omega_z & \omega_y \\ \omega_z & 0 & -\omega_x \\ -\omega_y & \omega_x & 0 \end{bmatrix} \tag{4.3}$$

is a skew symmetric matrix, that is, $\mathcal{S}^T = -\mathcal{S}$. The matrix $\mathcal{S}$ satisfies the relationship $\mathcal{S}(a)b = a \times b$, where a, b are arbitrary vectors and x denotes the cross product operation. Furthermore, $||\mathcal{S}(\boldsymbol{\omega})|| = ||\boldsymbol{\omega}||$.

4.2 Time-varying complementary filters. Navigation problem formulation.

We now extend the basic concepts of complementary filtering to the time-varying setting. The motivation for this work can be simply described by considering the example where one is interested in estimating the position $\mathbf{p}$ and velocity ${}^I\mathbf{v}$ of a vehicle based on measurements $\mathbf{p}_m$ and $\mathbf{v}_m$ of $\mathbf{p}$ and $\mathbf{v}$, respectively. In the case of an ocean surface vehicle, $\mathbf{p}_m$ is provided by a Differential Global Positioning System (SGPS), whereas $\mathbf{v}_m$ is provided by a Doppler sonar. In the case of a fully submerged underwater vehicle, $\mathbf{p}_m$ can be provided by a Long Baseline System.

It must be stressed that due to the physical characteristic of the Doppler sonar the *measurement* $\mathbf{v}_m$ *is naturally expresseed in body-axis, that is, in the reference frame* $\{\mathcal{B}\}$. Furthermore, Doppler bias effects are also naturally expressed in $\{\mathcal{B}\}$. This is in contrast with the measurements $\mathbf{p}_m$, which are directly available in the reference frame $\{\mathcal{I}\}$. These facts impose important constraints on the class of complementary filters for position and velocity estimation, as will become clear later.

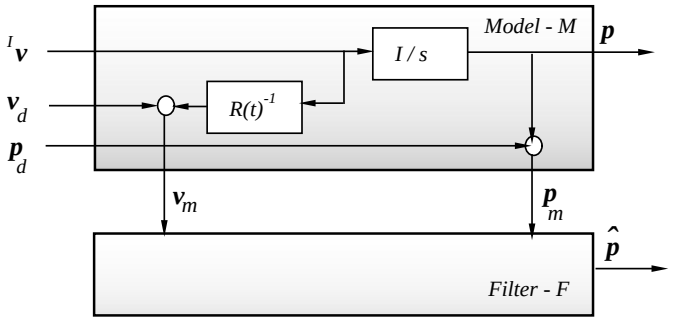

Figure 4.1: Process model.

The underlying process model $\mathcal{M}_{pv}$ is depicted in figure 4.1, where $\mathcal{F}$ is a dynamical system (filter) that operates on the measurements $\mathbf{p}_m$ and $\mathbf{v}_m$ to provide estimates $\hat{\mathbf{p}}$ of $\mathbf{p}$. In the figure, $\mathbf{p}_d$ and $\mathbf{v}_d$ are measurement disturbances. As in the last section, we study the situation where $\mathbf{p}_d = 0$ and $\mathbf{v}_d = \mathbf{v}_{d,0}$ where $\mathbf{v}_{d,0}$ is the Doppler bias. This set-up is all that is required for the design of complementary filters from a "frequency-like" domain point of view. Notice that the process model $\mathcal{M}_{pv}$ is time-varying due to the presence of the rotation matrix $R(t)$. However,the entries of $R(t)$ and their derivatives are not arbitrary functions of time but exhibit bounds that depend on each specific vehicle mission under consideration. For example, if an underwater vehicle motion is restricted to the horizontal plane and the maximum yaw rate achievable with that vehicle is r_{max}, then this information must be explicitly included in the description of the process model $\mathcal{M}_{pv}$ as we explain below. We now introduce the following definitions.

Definition. Process Model $\mathcal{M}_{pv}$. The process model $\mathcal{M}_{pv}$ is given by

$$\mathcal{M}_{pv} := \begin{cases} \dot{\mathbf{p}} &= \mathbf{v} \\ \mathbf{p}_m &= \mathbf{p} \\ \mathbf{v}_m &= \mathcal{R}^{-1}\mathbf{v} + \mathbf{v}_{d,0} \end{cases} \tag{4.4}$$

We further assume that the matrix $\mathcal{R}$ and its derivative $\dot{\mathcal{R}}$ are constrained through the inequalities

$$|\phi(t)| \leq \phi_{max}, |\theta(t)| \leq \theta_{max} \tag{4.5}$$

and

$$|p(t)| \leq p_{max}, |q(t)| \leq q_{max}, |q(t)| \leq r_{max} \tag{4.6}$$

for all $t \in \mathcal{R}_+$. Notice in the definition above that there are constraints on the roll and pitch angles ϕ and θ respectively, but not on the yaw angle ψ. This is due to the fact ocean vehicles are designed to undergo arbitrary maneuvers in yaw, but pitch and roll excursions are restricted by vehicle construction.

Definition. Candidate complementary filter. Consider the process model $\mathcal{M}_{pv}$ in (4.4) with $\mathbf{v}_{d,0}$ an arbitrary constant, and let $\mathcal{F}$ be a linear time-varying filter with realization

$$\mathcal{F} := \begin{cases} \dot{\mathbf{x}} &= A(t)\mathbf{x} + B_p(t)\mathbf{p}_m + B_v(t)\mathbf{v}_m \\ \hat{\mathbf{p}} &= C(t)\mathbf{x}. \end{cases} \tag{4.7}$$

Then, $\mathcal{F}$ is said to be a *candidate complementary filter* for $\mathcal{M}_{pv}$ if

- $\mathcal{F}$ is internally stable
- For every initial conditions $\mathbf{p}(0)$ and $\mathbf{x}(0)$, $\lim_{t\to\infty}\{\mathbf{p}(\mathbf{t}) - \hat{\mathbf{p}(\mathbf{t})}\} = 0$.
- $\mathcal{F}$ satisfies a bias rejection property, that is, $\lim_{t\to\infty} \hat{\mathbf{p}} = 0$ when $\mathbf{v} = 0$.

Definition. Complementary filter with break frequency ω_c. Let $\mathcal{F}$ be be a candidate complementary filter for $\mathcal{M}_{pv}$, and let $\mathcal{F}_p$ denote the corresponding operator from $\mathbf{p}_m$ to $\hat{\mathbf{p}}$. Then, $\mathcal{F}$ is said to be an (ϵ, n) *complementary filter* for $\mathcal{M}_{pv}$ with break frequency ω_c if $\mathcal{F}_p$ is an (ϵ, n) *low pass filter* with bandwidth ω_c.

The discussion in the previous sections leads directly to the following fiter design problem.

Problem formulation. *Given the process model $\mathcal{M}_{pv}$ in (4.4) and positive numbers ω_c, n, and ϵ, find an (ϵ, n) complementary fiter for $\mathcal{M}_{pv}$ with break frequency ω_c.*

5 Complementary filter design. Main results.

This section introduces a specific candidate complementary fiter structure for $\mathcal{M}_{pv}$ and derives sufficient conditions for the existence of a complementary filter with the structure adopted that meets required bandwith constraints.

5.1 Candidate complementary filter structure.

Figure 5.1 depicts the candidate filter structure for $\mathcal{M}_{pv}$ that will be adopted in the paper. The structure is motivated by the simple example described in Section 3, where an extra integrator

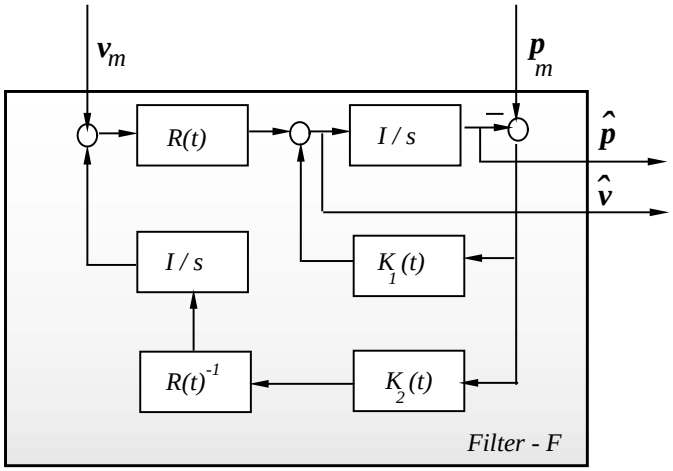

Figure 5.1: Complementary filter.

was inserted to estimate the rate gyro bias. Notice however that the filter explicitly includes the rotation matrix $\mathcal{R}(t)$, which we assume is available from an attitude reference system. The issue of robust filter performance against uncertainities in the measurement of $\mathcal{R}(t)$ will be addressed later in this section. In what follows, for simplicity of notation, we often avoid writing the explicit dependence of time-varying matrices on time. The following result is obtained.

Theorem 5.1 *Consider the process model $\mathcal{M}_{pv}$ and the time-varying filter*

$$\mathcal{F} := \begin{cases} \dot{\mathbf{x}}_1 &= R\mathbf{v}_m + R\mathbf{x}_2 + K_1(\mathbf{p} - \mathbf{x}_1) \\ \dot{\mathbf{x}}_2 &= R^{-1}K_2(\mathbf{p} - \mathbf{x}_1) \\ \hat{\mathbf{p}} &= \mathbf{x}_1 \end{cases} \tag{5.1}$$

Suppose the filter $\mathcal{F}$ is internally stable. Then, $\mathcal{F}$ is a candidate complementary filter for $\mathcal{M}_{pv}$.

Proof: From the assumptions, the time-varying filter has the realization

$$\mathcal{F} := \left[\begin{array}{c|c} A(t) & [B_p(t)\ B_v(t)] \\ \hline C(t) & 0 \end{array}\right],$$

where

$$A(t) = \begin{bmatrix} -K_1 & R \\ -\mathcal{R}^{-1}K_2 & 0 \end{bmatrix}, B_p(t) = \begin{bmatrix} K_1 \\ \mathcal{R}^{-1}K_2 \end{bmatrix}, B_v(t) = \begin{bmatrix} \mathcal{R} \\ 0 \end{bmatrix}, C(t) = \begin{bmatrix} I \\ 0 \end{bmatrix}$$

Furthermore, $\mathbf{v}_m = \mathbf{v} + \mathbf{v}_{d,0}$, where $\mathbf{v}_{d,0}$ is an arbitrary constant vector (Doppler bias). Let $\Phi(t,\tau)$ denote the state transition matrix associated with $A(t)$. Then, using the equalities

$$B_P\mathbf{p}(\tau) = -A(\tau)\begin{bmatrix} \mathbf{p}(\tau) \\ 0 \end{bmatrix}, B_v\mathbf{v}(\tau) = \begin{bmatrix} \frac{d}{d\tau}\mathbf{p}(\tau) \\ 0 \end{bmatrix}, B_v\mathbf{v}_{d,0} = -A(\tau)\begin{bmatrix} 0 \\ \mathbf{v}_{d,0} \end{bmatrix}$$

the filter state evolution is given by

$$\begin{aligned}
\begin{bmatrix} \mathbf{x}_1(t) \\ \mathbf{x}_2(t) \end{bmatrix} &= \Phi(t,t_0) \begin{bmatrix} \mathbf{x}_1(t_0) \\ \mathbf{x}_2(t_0) \end{bmatrix} + \int_{t_0}^{t} \Phi(t,\tau) \left\{ B_P \mathbf{p}(\tau) + B_v(\mathbf{v}(\tau) + \mathbf{v}_{d,0}) \right\} d\tau \\
&= \Phi(t,t_0) \begin{bmatrix} \mathbf{x}_1(t_0) \\ \mathbf{x}_2(t_0) \end{bmatrix} \\
&+ \int_{t_0}^{t} \Phi(t,\tau) \left\{ -A(\tau) \begin{bmatrix} \mathbf{p}(\tau) \\ 0 \end{bmatrix} + \begin{bmatrix} \frac{d}{d\tau}\mathbf{p}(\tau) \\ 0 \end{bmatrix} \right\} d\tau \\
&+ \int_{t_0}^{t} \Phi(t,\tau) \left\{ -A(\tau) \begin{bmatrix} 0 \\ \mathbf{v}_{d,0} \end{bmatrix} \right\} d\tau
\end{aligned} \tag{5.2}$$

The transition matrix $\Phi(t,\tau)$ satisfies

$$\frac{d}{d\tau}\Phi(t,\tau) = -\Phi(t,\tau)A(\tau) \tag{5.3}$$

and therefore 5.2 can also be written as

$$\begin{aligned}
\begin{bmatrix} \mathbf{x}_1(t) \\ \mathbf{x}_2(t) \end{bmatrix} &= \Phi(t,t_0) \begin{bmatrix} \mathbf{x}_1(t_0) \\ \mathbf{x}_2(t_0) \end{bmatrix} + \int_{t_0}^{t} \left\{ \frac{d}{d\tau} \left(\Phi(t,\tau) \begin{bmatrix} p(\tau) \\ 0 \end{bmatrix} \right) \right\} d\tau \\
&+ \int_{t_0}^{t} \left\{ \frac{d}{d\tau} \left(\Phi(t,\tau) \begin{bmatrix} 0 \\ \mathbf{v}_{d,0} \end{bmatrix} \right) \right\} d\tau \\
&= \Phi(t,t_0) \begin{bmatrix} \mathbf{x}_1(t_0) \\ \mathbf{x}_2(t_0) \end{bmatrix} + \begin{bmatrix} \mathbf{p}(t) \\ 0 \end{bmatrix} - \Phi(t,t_0) \begin{bmatrix} \mathbf{p}(t_0) \\ 0 \end{bmatrix} \\
&+ \begin{bmatrix} 0 \\ \mathbf{v}_{d,0} \end{bmatrix} - \Phi(t,t_0) \begin{bmatrix} 0 \\ \mathbf{v}_{d,0} \end{bmatrix}
\end{aligned} \tag{5.4}$$

Since the filter is stable, $\lim_{t\to\infty} ||\Phi(t,t_0)|| = 0$. The results follows immediately by observing that $\hat{\mathbf{p}} = \mathbf{x}_1$. ■

Notice that the state $\mathbf{x}_2$ of the appended integrator tends asymptotically to $-\mathbf{v}_{d,0}$. Thus, $\mathbf{x}_2$ provides an estimate of the Doppler bias in the body frame. This result makes perfect sense form a physical point of view since the bias is constant in the body frame (not in the reference frame $\mathcal{I}$).

5.2 The candidate complementary filter: sufficient conditions for stability and guaranteed break frequency.

The next result establishes sufficient conditions for the existence of fixed gains K_1 and K_2 such that the candidate filter is internally stable and has a a guaranteed break frequency of at least ω_c, where ω_c is a design parameter. In preparation for that result we let

$$\boldsymbol{\omega}_r = [p_r \; q_r \; r_r \;]^T := \mathcal{R}\boldsymbol{\omega}$$

and define

$$\mathcal{S}_r := S(\boldsymbol{\omega}_r) = S(\mathcal{R}\boldsymbol{\omega})$$

Given the original design bounds (4.5)-(4.6), it is possible to compute positive upper bounds p_r^+, q_r^+, and r_r^+ such that

$$|p_r| \leq p_r^+, |q_r| \leq q_r^+, |r_r| \leq r_r^+. \tag{5.5}$$

Let $p_r^- = -p_r^+, q_r^- = -q_r^+, r_r^- = -r_r^+$ and construct the set $\{\boldsymbol{\omega}_r^i, i = \{1,..,8\}\}$, where

$$\boldsymbol{\omega}_r^1 = \begin{bmatrix} p_r^- \\ q_r^- \\ r_r^- \end{bmatrix}, \boldsymbol{\omega}_r^2 = \begin{bmatrix} p_r^+ \\ q_r^- \\ r_r^- \end{bmatrix}, \boldsymbol{\omega}_r^3 = \begin{bmatrix} p_r^- \\ q_r^+ \\ r_r^- \end{bmatrix}, \boldsymbol{\omega}_r^4 = \begin{bmatrix} p_r^+ \\ q_r^+ \\ r_r^- \end{bmatrix}, ...\boldsymbol{\omega}_r^8 = \begin{bmatrix} p_r^+ \\ q_r^+ \\ r_r^+ \end{bmatrix}.$$

Then

$$\boldsymbol{\omega}_r \in \mathbf{Co}\{\boldsymbol{\omega}_r^i, i = \{1,..,8\}\} \text{ and}$$
$$\mathcal{S}_r \in \mathbf{Co}\{\mathcal{S}_r^i = \mathcal{S}(\boldsymbol{\omega}_r^i);\; i = \{1,..,8\}\}$$

Theorem 5.2 *Consider the linear time-varying filter (5.1) and assume that the bounds (5.5) on $\boldsymbol{\omega}_r$ apply. Given n and ω_c, let*

$$\mathcal{W}_{\omega_c}^n := \left[\begin{array}{c|c} A_W & B_W \\ \hline C_W & 0 \end{array}\right]$$

be a minimal realization for the weighting Chebyschev filter introduced in Section 3.2. Further let

$$F = \begin{bmatrix} 0 & I \\ 0 & \mathcal{S}_r \end{bmatrix}, \quad H = [-I \;\; 0].$$

Suppose that given $\epsilon > 0$ $\exists$ $K \in \mathcal{R}^{6\times 3}$, $P \in \mathcal{R}^{(6+n)\times(6+n)}$, $P > 0$, *such that the* linear matrix inequalities

$$L_{LP_i}(K,P,\epsilon) := \left[\begin{array}{c|c} P\begin{bmatrix} F_i + KH & KC_W \\ 0 & A_W \end{bmatrix} + \begin{bmatrix} F_i + KH & KC_W \\ 0 & A_W \end{bmatrix}^T P + \begin{bmatrix} H^T \\ -C_W^T \end{bmatrix}[H \quad -C_W] & P\begin{bmatrix} 0 \\ B_W \end{bmatrix} \\ \hline \begin{bmatrix} 0 & B_W^T \end{bmatrix} P & -\epsilon^2 I \end{array}\right] < 0,$$

$$F_i = \begin{bmatrix} 0 & I \\ 0 & \mathcal{S}(\boldsymbol{\omega}_r^i) \end{bmatrix}, \quad i = \{1, ...8\} \tag{5.6}$$

are satisfied. Then, the constant gains

$$\begin{bmatrix} K_1 \\ K_2 \end{bmatrix} := K$$

make the filter $\mathcal{F}$ *internally stable. Furthermore, the operator* $\mathcal{F}_p : \mathbf{p} \to \hat{\mathbf{p}}$ *satisfies a low pass property with indices* (ϵ, n) *over* $[0, \omega_c]$, *that is,* $||(\mathcal{F}_p - I)\mathrm{W}_{\omega_c}^n|| < \epsilon$.

Proof: Given the realization 5.1, consider the Lyapunov coordinate transformation [5]

$$\boldsymbol{\zeta}(t) = \bar{P}(t)\mathbf{x}(t),$$

where

$$\bar{P}(t) = \begin{bmatrix} I & 0 \\ 0 & R(t) \end{bmatrix}.$$

With this change of coordinates, the operator $\mathcal{F}_p$ admits the realization

$$\mathcal{F}_p = \begin{cases} \dot{\boldsymbol{\zeta}} &= (\bar{P}A\bar{P}^{-1} + \dot{\bar{P}}\bar{P}^{-1})\boldsymbol{\zeta} + \bar{P}B_p\mathbf{p} \\ \hat{\mathbf{p}} &= C\bar{P}^{-1}\boldsymbol{\zeta} \end{cases} \tag{5.7}$$

Using the relations

$$\bar{P}A\bar{P}^{-1} = \begin{bmatrix} -K_1 & I \\ -K_2 & 0 \end{bmatrix}$$

and

$$\dot{\bar{P}}\bar{P}^{-1} = \begin{bmatrix} 0 & 0 \\ 0 & \mathcal{R}\mathcal{S}(\boldsymbol{\omega})\mathcal{R}^{-1} \end{bmatrix} = \begin{bmatrix} 0 & 0 \\ 0 & \mathcal{S}(\mathcal{R}\boldsymbol{\omega}) \end{bmatrix} = \begin{bmatrix} 0 & 0 \\ 0 & \mathcal{S}(\boldsymbol{\omega}_r) \end{bmatrix}$$

(5.7) can be written as

$$\begin{aligned}\dot{\boldsymbol{\zeta}} &= \begin{bmatrix} -K_1 & I \\ -K_2 & \mathcal{S}(\boldsymbol{\omega}_r) \end{bmatrix} \boldsymbol{\zeta} + \begin{bmatrix} K_1 \\ K_2 \end{bmatrix} \mathbf{p} \\ \hat{\mathbf{p}} &= [I \;\; 0]\, \boldsymbol{\zeta} \end{aligned} \tag{5.8}$$

Simple algebra now shows that $(\mathcal{F}_p - I)\, W_{\omega_c}^n$ admits the state-space representation

$$(\mathcal{F}_p - I)\, W_{\omega_c}^n := \left[\begin{array}{ccc|c} -K_1 & I & K_1 C_W & 0 \\ -K_2 & \mathcal{S}_r & K_2 C_W & 0 \\ 0 & 0 & A_W & B_W \\ \hline I & 0 & -C_W & 0 \end{array}\right] \tag{5.9}$$

$$\begin{aligned} &= \left[\begin{array}{cc|c} F + KH & KC_W & 0 \\ 0 & A_W & B_W \\ \hline H & -C_W & 0 \end{array}\right] \\ &\in \mathbf{Co}\left\{ \left[\begin{array}{cc|c} F_i + KH & KC_W & 0 \\ 0 & A_W & B_W \\ \hline H & -C_W & 0 \end{array}\right], i = \{1, ..., 8\} \right\}. \end{aligned}$$

where

$$K = \begin{bmatrix} K_1 \\ K_2 \end{bmatrix}$$

and F, H, and F_i are defined above.

Suppose $\exists\; P > 0$ and K such that

$$\left[\begin{array}{c|c} P \begin{bmatrix} F_i + KH & KC_W \\ 0 & A_W \end{bmatrix} + \begin{bmatrix} F_i + KH & KC_W \\ 0 & A_W \end{bmatrix}^T P + \begin{bmatrix} H^T \\ -C_W^T \end{bmatrix} [H \;\; -C_W] & P \begin{bmatrix} 0 \\ B_W \end{bmatrix} \\ \hline \begin{bmatrix} 0 & B_W^T \end{bmatrix} P & -\epsilon^2 I \end{array}\right] < 0, \tag{5.10}$$

$i = \{1, ..., 8\}$.

Then, using standard results on polytopic system analysis (see equation (6.54) in [3])) it follows that $||(\mathcal{F}_p - I)\, W_{\omega_c}^n|| < \epsilon$. Clearly, if the inequalities (5.10) are satisfied then the gains

$$\begin{bmatrix} K_1 \\ K_2 \end{bmatrix} := K \tag{5.11}$$

guarantee that $||(\mathcal{F}_p - I)\, W_{\omega_c}^n|| < \epsilon$. Notice if expression (5.10) is satisfied for some P and K then the matrices

$$\begin{bmatrix} F_i + KH & KC_W \\ 0 & A_W \end{bmatrix}$$

are stable $\forall i = \{1, ...8\}$ and therefore the polytopic system (5.8) with state matrix $F + KH$ is internally stable [3]. Since Lyapunov transformations preserve internal stability, the original system 5.1 is also internaly stable.

■

The above theorem establishes sufficient conditions for the existence of fixed gains K_1 and K_2 such that the complementary filter (5.1) is internally stable and meets desired "frequency-like" response characteristics. However, it does not provide any results on the feasibility of the problem at hand. The theorem that follows addresses this problem partially, by showing that there always exists a set of fixed gains for which the filter (5.1) is internally stable.

Theorem 5.3 *Consider the linear time-varying filter (5.1). Then, for every set of finite positive numbers p_r^+, q_r^+, and r_r^+ such that the bounds (5.5) on $\boldsymbol{\omega}_r$ apply there exist fixed gains K_1 and K_2 that make the filter internaly stable.*

Proof: From the proof of Theorem 5.2, the filter (5.1) is internally stable if and only if the unforced polytopic sytem

$$\dot{\boldsymbol{\zeta}} = (F + KH)\boldsymbol{\zeta} \tag{5.12}$$

is internally stable for some choice of K. Given (5.12), consider the related time-invariant system

$$\dot{\boldsymbol{\zeta}} = (A + KH)\boldsymbol{\zeta} = A_K\boldsymbol{\zeta}, \tag{5.13}$$

where

$$A_K = A + KH;\ A = \begin{bmatrix} 0 & I \\ 0 & 0 \end{bmatrix}.$$

The simple structures of the matrices A and H implies that (5.13) can be made stable by chosing $K_1 = k_1 I, K_2 = k_2 I$, where k_1 and $k_2 > 0$ are positive but otherwise arbitrary. This stems from the fact that the closed loop eigenvalues of $A + KH$ have multipliciy three and are easily obtained from the roots of the second order polynomial $s^2 + k_1 s + k_2$. Therefore, from basic Lyapunov stability theory it follows that for every $\gamma_1 > 0, \gamma_2 > 0$ there exists a positive definite matrix

$$P_1 = \begin{bmatrix} P_{11} & P_{12} \\ P_{12} & P_{22} \end{bmatrix} > 0$$

such that

$$A_K^T P_1 + P_1 A_K = -Q = \begin{bmatrix} -\gamma_1 I & 0 \\ 0 & -\gamma_2 I \end{bmatrix} \tag{5.14}$$

Expanding (5.14) we obtain

$$\left[\begin{array}{c|c} -2P_{11}K_1 - 2P_{12}K_2 & -P_{12}K_1 - P_{22}K_2 + P_{11} \\ \hline (-P_{12}K_1 - P_{22}K_2 + P_{11})^T & 2P_{12} \end{array}\right] = \begin{bmatrix} -\gamma_1 I & 0 \\ 0 & -\gamma_2 I \end{bmatrix} \tag{5.15}$$

and therefore $P_{12} = -(\gamma_2/2)I$. Furthermore, since K_1 and K_2 are diagonal, P_{11} and P_{22} are also diagonal. Consider now the linar time-invariant systems

$$\dot{\boldsymbol{\zeta}} = (F_i + KH)\boldsymbol{\zeta} = A_{K_i}\boldsymbol{\zeta};\ i = 1, 2, ..., 8 \tag{5.16}$$

with F_i defined as before. Using the relation $(\mathcal{S}_r^i)^T = -\mathcal{S}_r^i$ it follows that

$$A_{K_i} P_1 + P_1 A_{K_i} = \begin{bmatrix} -\gamma_1 I & P_{12}\mathcal{S}_r^i \\ (\mathcal{S}_r^i)^T P_{12} & -\gamma_2 I \end{bmatrix};\ i = 1, 2, ..., 8 \tag{5.17}$$

We now show that (5.17) can be made negative definite for all $i = 1, 2, ...8$ by suitable choice of γ_1 and γ_2. In fact, using Schur complements [3] it easily shown that (5.17) is negative definite if and only if

$$\gamma_1 I - P_{12}\mathcal{S}_r^i \gamma_2^{-1} (\mathcal{S}_r^i)^T P_{12} = \gamma_1 I - (\gamma_2/4)\mathcal{S}_r^i (\mathcal{S}_r^i)^T > 0.$$

Since $||S_r^i(\boldsymbol{\omega}_r^i)|| = ||\boldsymbol{\omega}_r^i||$, the above expression is satisfied with $\gamma_2 = 4$ and $\gamma_1 > \max\{||\boldsymbol{\omega}_r^i||^2 : i = 1, 2, ...8\}$. Hence, using the theory of polytopic systems [3] the system (5.12) and therefore the original complementary filter are internally stable. ■

Note. From the proof of the theorem, it follows that the linear time-varying filter (5.1) is internally stable for any choice of constant, positive, diagonal matrices K_1 and K_2.

We now address the issue of performance robustness of the complementary filter in the presence of measurement errors in the rotation matrix $\mathcal{R}$. In what follows, we let $\mathcal{R} = \mathcal{R}(\boldsymbol{\lambda})$ and $\mathcal{R}_m = \mathcal{R}_m(\boldsymbol{\lambda}_m)$ denote the "true" and measured rotation matrices, which are functions of the "true" and measured orientation vectors $\boldsymbol{\lambda}$ and $\boldsymbol{\lambda}_m$, respectively. We further let $\mathcal{R} - \mathcal{R}_m = \Delta\mathcal{R}$ and assume that $\Delta\mathcal{R}$ is bounded, that is, there exists a positive constant δ_R such that $||\Delta\mathcal{R}|| \leq \delta_R$.

To compute the influence of $\Delta\mathcal{R}$ on the estimation error $\mathbf{e}_p = \mathbf{p} - \hat{\mathbf{p}}$, we set $\mathbf{p}_m = \mathbf{p}$ and $\mathbf{v}_m = \mathbf{v}$. From (4.4) and (5.1) it follows that the error $\mathbf{e}_p$ is the output of a dynamical system with input $\mathbf{v}$ and state space realization

$$\mathcal{F}_e := \left[\begin{array}{cc|c} -K_1 & \mathcal{R}_m & \Delta\mathcal{R} \\ -\mathcal{R}_m^{-1}K_2 & 0 & 0 \\ \hline I & 0 & 0 \end{array}\right] \tag{5.18}$$

The state matrix of $\mathcal{F}_e$ equals that of $\mathcal{F}$ in Theorem 5.1. Therefore, internal stability is obtained if the conditions of Theorem 5.2 are met with $\mathcal{R}$ replaced by $\mathcal{R}_m$. In particular, if the filter gains K_1 and K_2 are constant, diagonal, and positive then internal stability is automatically ensured (see Theorem 5.3). The issue of robust performance requires further thought, but can be addressed by viewing $\mathcal{F}_e$ as an input-output operator with realization

$$\bar{\mathcal{F}}_e := \left[\begin{array}{cc|c} -K_1 & \mathcal{R}_m & I \\ -\mathcal{R}_m^{-1}K_2 & 0 & 0 \\ \hline I & 0 & 0 \end{array}\right] \tag{5.19}$$

and input $\mathbf{u} = \Delta\mathcal{R}\mathbf{v}$. If $\mathbf{v}$ is bounded uniformly in time, that is, $||\mathbf{v}||_\infty = \mathbf{v}_\infty < \infty$ then

$$||\mathbf{u}||_\infty \leq ||\Delta\mathcal{R}||||\mathbf{v}||_\infty = \delta_R \mathbf{v}_\infty$$

Since $\bar{\mathcal{F}}_e$ is internally stable, the induced norm $||\bar{\mathcal{F}}_e|_{\infty,i}$ of the corresponding operator is finite. Therefore,

$$||\mathbf{e}(t)||_2 \leq ||\mathbf{e}||_\infty \leq ||\bar{\mathcal{F}}_e||_{\infty,i}\ \delta_R \mathbf{v}_\infty$$

for all t in $\mathcal{R}_+$. Thus, *the estimation error* $\mathbf{e(t)}$ *remains bounded for all* t *in the presence of measurement errors in* $\mathcal{R}$ *and decreases uniformly to zero as* δ_R *approaches zero.*

From the discussion above, it follows that the induced operator norm $||\bar{\mathcal{F}}_e||_{\infty,i}$ is the correct measure of performance robustness of the filter against measurement perturbations in the rotation matrix $\mathcal{R}$. A constraint on $||\bar{\mathcal{F}}_e||_{\infty,i}$ can be included in the filter design process by using the circle of ideas discussed in [20].

6 Filter Design: a practical algorithm. Simulation results.

The previous section introduced the mathematical tools that are required to design a candidate complementary filter with a guaranteed break frequency. Notice, however, that the outcome of the design process may very well be a filter with an effective bandwith that is greater than the one required. Clearly, the set of possible solutions must be further constrained so that the designer have an extra design parameter at his disposal to select one solution (if it exists) that meets the required break frequency criterion. This situation is identical to what happens in the case of filter design using Kalman-Bucy theory, where the noise covariances play the role of "tuning knobs" to shape the filter characteristics.

In the linear time-invariant case, a simple analysis of a Bode diagram indicates that an expedite way of setting an upper bound on the break frequency is to make the filter "roll-off" sufficiently fast. In the time-varying setting, this corresponds to making $||\mathcal{F}_p \mathcal{W}_{\omega_t}^{n_t}|| < \gamma$, where $\mathcal{W}_{\omega_t}^{n_t}$ is a high

pass Chebyshev filter and ω_t and γ play the role of "tuning parameters". In practice, it is sufficient to vary the value of of the parameter γ.

These considerations lead directly to a *practical algorithm* for the *design* of a time-varying complementary filter with a desired break frequency ω_c. This is done by using theorem 5.11 with the additional "high-frequency" constraint described above, which can be also cast as a Linear matrix Inequality. The underlying optimization problem can be formulated as follows:

$$\begin{aligned}
&\min_K \gamma \\
&\text{subject to} \\
&||(I - \mathcal{F}_p)\mathcal{W}^n_{\omega_{0c}}|| < \epsilon_0 \\
&||\mathcal{F}_p\mathcal{W}^{n_t}_{\omega_t}|| < \gamma,
\end{aligned} \tag{6.1}$$

where the minimization is performed over the the set of gain matrices $K \in \mathcal{R}^{6x3}$ and ϵ_0 captures the low-pass requirement constraint. It is simple to see that the high-pass constraint $||\mathcal{F}_p\mathcal{W}^{n_t}_{\omega_t}|| < \gamma$ is satisfied if $\exists\ Y > 0$ and K such that

$$L_{HP_i}(Y,K,\gamma) := \left[\begin{array}{c|c} Y\begin{bmatrix} F_i + KH & KC_{W_t} \\ 0 & A_{W_t} \end{bmatrix} + \begin{bmatrix} F_i + KH & KC_{W_t} \\ 0 & A_{W_t} \end{bmatrix}^T Y & Y\begin{bmatrix} KD_{W_t} \\ B_{W_t} \end{bmatrix} \\ + \begin{bmatrix} H^T \\ 0 \end{bmatrix}[H \ \ 0] & \\ \hline \begin{bmatrix} KD_{W_t} & B^T_{W_t} \end{bmatrix} Y & -\gamma^2 I \end{array}\right] < 0, \tag{6.2}$$

$$i = \{1, ...8\},$$

where

$$\mathcal{W}^{n_t}_{\omega_t} = \left[\begin{array}{c|c} A_{W_t} & B_{W_t} \\ \hline C_{W_t} & D_{W_t} \end{array}\right].$$

The optimization problem (6.1) can now be cast in the LMI framework as follows. For given numbers $\epsilon > 0$ and $\gamma > 0$ define the sets

$$\Phi_{LP}(\epsilon) = \{K, P : P > 0, L_{LP_i}(K,P,\epsilon) < 0, \forall i = 1, ..., 8\}, \tag{6.3}$$

$$\Phi_{HP}(\gamma) = \left\{K, Y : Y > 0, L_{HP_j}(K,Y,\gamma) < 0, \forall j = 1, ..., 8\right\}, \tag{6.4}$$

where the expressions $L_{LP_i}(K,P,\epsilon)$ and $L_{HP_j}(K,Y,\gamma)$ were defined in (5.6) and (6.2), respectively. Then the solution K to the optimization problem (6.1) can be obtained by solving the following constrained optimization problem:

$$\min_{(K,P)\in\Phi_{LP}(\epsilon_0);(K,Y)\in\Phi_{HP}(\gamma)} \gamma. \tag{6.5}$$

The optimization problem (6.5) is nonconvex. However, the matrix inequalities $L_{LP_i}(K,P,\epsilon) < 0$ and $L_{HP_j}(K,Y,\gamma) < 0$ are jointly linear in the parameters P, K and Y. Therefore, for fixed K the expressions $L_{LP_i}(K,P,\epsilon)$ and $L_{HP_j}(K,Y,\gamma)$ are linear in P and Y respectively, and for fixed P and Y they are linear in K. This observation suggests the following numerical solution/design procedure to solve the above constrained optimization problem (see [9] and references therein for similar approaches reported in the literature):

I Initializiation

1 Fix $\epsilon > \epsilon_0 > 0$. From operational conditions, determine the operating range of angular velocities p_r, q_r, r_r:

$$|p_r| \leq p_r^+, |q_r| \leq q_r^+, |r_r| \leq r_r^+.$$

2 Specify the frequency ω_c and use it to construct the low-pass weight $\mathcal{W}_{\omega_c}^n$.

3 Specify the bandwidth ω_t of the high-pass weight $\mathcal{W}_{\omega_t}^{n_t}$. (As a rule-of-thumb choose $\omega_t >> \omega_c$).

4 Select initial values for the gains K_1, K_2. (As suggested by the theorem 5.3 any gains of the form $\gamma_1 I$, $\gamma_2 I$, $\gamma_1 > 0$, $\gamma_2 > 0$ will do.)

II Numerical optimization

1 Low-pass constraint. Solve

$$\min_{(P,K)\in\Phi_{LP}(\epsilon),\epsilon\geq\epsilon_0} \epsilon. \tag{6.6}$$

Use $K = [\gamma_1^T \ \gamma_2^T]$ obtained in step I.4 to initialize K, then iterate over P and K to solve the optimization problem (6.6). If no solution is found, increase ϵ_0.

2 High-pass constraint. Let (P^*, K^*) denote the solution to the optimization problem (6.6). Solve

$$\min_{(Y,K)\in\Phi_{HP}(\gamma),(P^*,K)\in\Phi_{LP}(\epsilon_0)} \gamma. \tag{6.7}$$

Use K^* as an initial value for K, then iterate over Y and K to solve the optimization problem (6.7).

Due to nonconvexity the numerical solutions proposed in Steps II.1 and II.2 are not guaranteed to converge to a local minimum [9]. Therefore, the algorithm should be run for multiple initial conditions. It is then up to the system designer to select appropriate values of the tuning parameters to try and meet all the criteria that must be satisfied by a complementary filter with a desired break

frequency. See the definitions of *complementary filter with break frequency* ω_c and *low pass filter with bandwidth* ω_c introduced early in the paper.

To illustrate the performance of the complementary filtering structure, a simple filter design exercise was carried out for an autonomous surface vehicle undergoing rotational maneuvers in the horizontal plane. In this case, the navigation system is required to provide accurate estimates of the vehicle's position based on position and velocity measurements provided by a DGPS and a Doppler sonar, respectively. In the scenario adopted the vehicle progresses at a constant speed of $2m/s$ while it executes repeated turns at a maximum yaw rate of $3rad/s$. The Doppler sonar is assumed to introduce a constant bias term $\mathbf{v}_{d,0} = [0.1m/s,\ 0.2m/s]^T$. The selected break frequency for the complementary filter was $\omega_c = 0.4rad/s$.

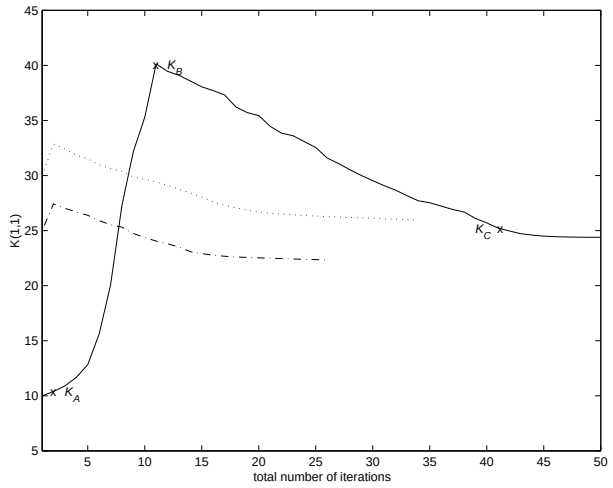

Figure 6.1: Filter gain K(1,1) versus iteration number.

The design procedure is illustrated in figures 6.1 - 6.3. In the design, the orders n and n_t of the Chebyschev weights $\mathcal{W}_{\omega_c}^n$ and $\mathcal{W}_{\omega_t}^{n_t}$ were selected as 2. Furthermore, ω_t was set arbitrarily to $60rad/s$. The performance parameter ϵ_0 for the low pass filter was chosen as 0.2.

Figure 6.1 shows the evolution of the complementary filter gain $K(1,1)$ for three different initial values. The bold curve shows clearly the general tendency for the case where the initial values are small: the filter does not exhibit a high enough break frequency, and therefore the gains are increased until the low pass requirement is met, possibly with a certain margin (the margin depends on the particular sequence of iterations obtained by running the first minimization problem in (6.6)). At this point, the high-pass constraint comes into play, forcing the gains to change until the low-pass constraint is met, without incurring too much spillover at high frequencies.

The three lower curves in figure 6.2 are plots of $||(\mathcal{F}_p - I)\mathcal{W}_{\omega_c}^n||$ as a function of ω_c, the operator $\mathcal{F}_p$ being computed with the gains obtained at steps A, B, and C of figure 6.1. The top curve I

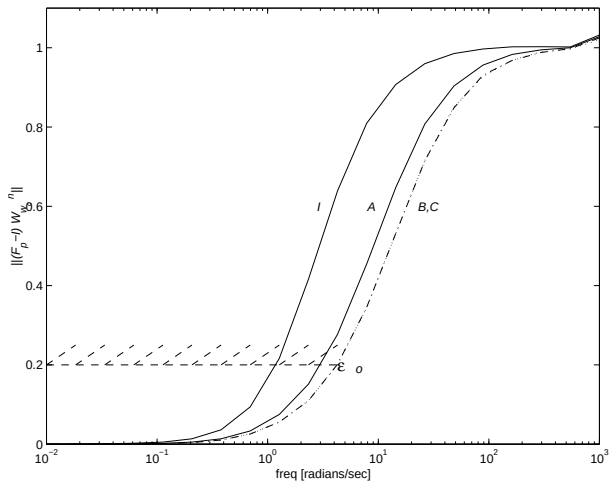

Figure 6.2: Generalized bode plots - low pass property

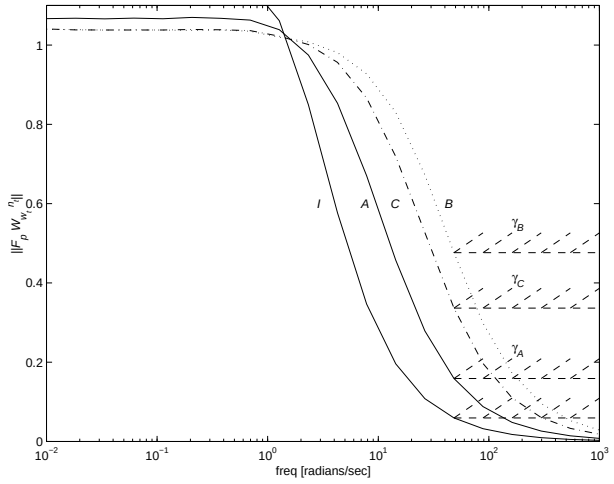

Figure 6.3: Generalized bode plots - high pass property

shows the case where the filter gains were set to values much smaller than those obtained in step A. Henceforth, we will refer to such plots as *generalized Bode plots.* The figure shows clearly that the filter starts with a break frequency that is smaller than that required, that frequency being increased until the break frequency requirement is met. It is the role of the "high-pass" constraint to guarantee that the low-pass requirement be met while reducing the spillover at high frequencies. Figure 6.3 shows the evolution of $||(\mathcal{F}_p)\mathcal{W}_{\omega_t}^{n_t}||$ as a function of ω_t. The iterative procedure described above aims at minimizing the value γ of these generalized Bode plots at $\omega = 60 rad/s$ subject to the low pass constraint described before. The cases I and A violate the low pass constraint and are therefore not important to examine. Notice, however, how the value of γ decreases from iteration B to C, thus showing that in case C less spillover is introduced at high frequency.

The performance of the resulting filter was assessed in simulation. Figure 6.4 shows the actual and estimated vehicle position when the initial state of the filter was set to $\mathbf{x}_1 = [10m,\ 20m]^T$ and $\mathbf{x}_2 = [0m/s,\ 0m/s]^T$. Figure 6.5 captures the evolution of the first component of the Doppler bias estimate. It can be concluded from the figures that the filter provides good tracking of the actual inertial trajectory and rejects the bias introduced by the Doppler unit in the body-axis.

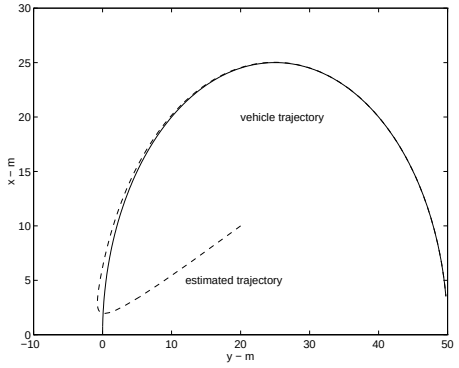

Figure 6.4: Actual and estimated vehicle trajectory.

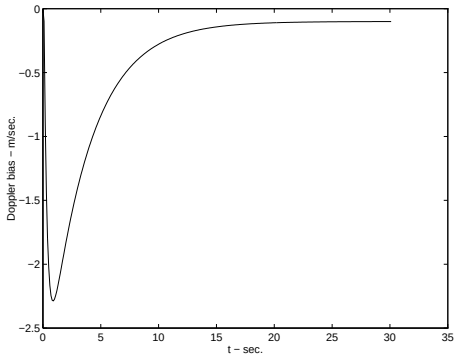

Figure 6.5: - Doppler bias esimate.

7 Extension to Accelerometers

In this section we extend the results discussed above to include the case of complementing position information with that available from onboard accelerometers. This is a scenario commonly encountered in the case of air vehicles. First, we introduce additional notation:

- ${}^I\mathbf{a}$ - linear acceleration of the origin of $\{\mathcal{B}\}$ measured in $\{\mathcal{I}\}$.
- $\mathbf{a}$ - linear acceleration of the origin of $\{\mathcal{B}\}$ with respect to $\{\mathcal{I}\}$, resolved in $\{\mathcal{B}\}$

Using this notation we establish the following kinematic relationships for the case of accelerometers:

$$\dot{\mathbf{p}} = {}^{I}\mathbf{v} \tag{7.1}$$

$${}^{I}\dot{\mathbf{v}} = {}^{I}\mathbf{a} = \mathcal{R}\mathbf{a} \tag{7.2}$$

$$\dot{\mathcal{R}} = \mathcal{R}S(\boldsymbol{\omega}), \tag{7.3}$$

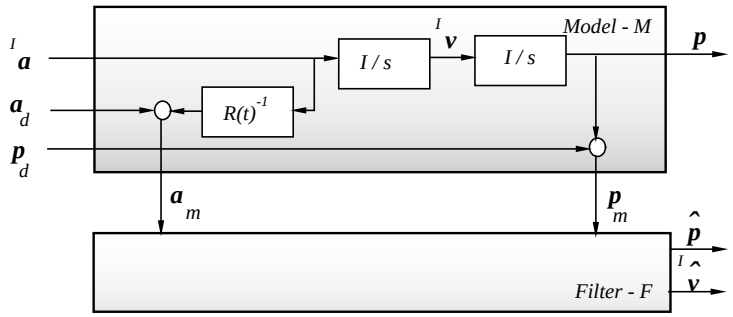

Figure 7.1: Process model $\mathcal{M}_{pa}$

The underlying process model $\mathcal{M}_{pa}$ is depicted in figure 7.1, where $\mathcal{F}$ is a dynamical system (filter) that operates on the measurements $\mathbf{p}_m$ and $\mathbf{a}_m$ to provide estimates $\hat{\mathbf{p}}$ of $\mathbf{p}$. In the figure, $\mathbf{p}_d$ and $\mathbf{a}_d$ are measurement disturbances. As in section 5, we study the situation where $\mathbf{p}_d = 0$ and $\mathbf{a}_d = \mathbf{a}_{d,0}$ where $\mathbf{a}_{d,0}$ is the accelerometer bias.

Definition. Process Model $\mathcal{M}_{pa}$. The process model $\mathcal{M}_{pa}$ is given by

$$\mathcal{M}_{pa} := \begin{cases} \dot{\mathbf{p}} &= {}^{I}\mathbf{v} \\ {}^{I}\dot{\mathbf{v}} &= {}^{I}\mathbf{a} \\ \mathbf{p}_m &= \mathbf{p} \\ \mathbf{a}_m &= \mathcal{R}^{-1}\,{}^{I}\mathbf{a} + \mathbf{a}_{d,0} \end{cases} \tag{7.4}$$

The discussion in the previous sections leads directly to the following fiter design problem.

Problem formulation. *Given the process model $\mathcal{M}_{pa}$ in (7.4) and positive numbers ω_c, n, and ϵ, find an (ϵ, n) complementary fiter for $\mathcal{M}_{pa}$ with break frequency ω_c.*

The theorem that follows introduces a candidate complementary filter for $\mathcal{M}_{pa}$ (see Figure 7.2). The filter structure is motivated by the results presented in previous sections, where an extra integrator was inserted to estimate the Doppler bias.

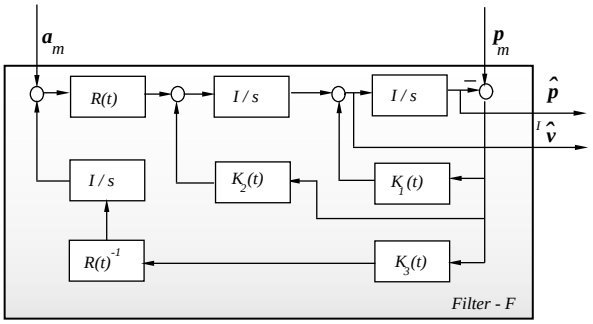

Figure 7.2: Complementary filter $\mathcal{F}_a$.

Theorem 7.1 *Consider the process model $\mathcal{M}_{pa}$ and the time-varying filter*

$$\mathcal{F} := \begin{cases} \dot{\mathbf{x}}_1 &= \mathbf{x}_2 + K_1(\mathbf{p} - \mathbf{x}_1) \\ \dot{\mathbf{x}}_2 &= R\mathbf{a}_m + R\mathbf{x}_3 + K_2(\mathbf{p} - \mathbf{x}_1) \\ \dot{\mathbf{x}}_3 &= R^{-1}K_3(\mathbf{p} - \mathbf{x}_1) \\ \hat{\mathbf{p}} &= \mathbf{x}_1 \end{cases} \tag{7.5}$$

Suppose the filter $\mathcal{F}$ is internally stable. Then, $\mathcal{F}$ is a candidate complementary filter for $\mathcal{M}_{pa}$.

The next result establishes sufficient conditions for the existence of fixed gains K_1, K_2 and K_3 such that the candidate filter is internally stable and has a a guaranteed break frequency of at least ω_c, where ω_c is a design parameter.

Theorem 7.2 *Consider the linear time-varying filter (7.5) and assume that the bounds (5.5) on $\boldsymbol{\omega}_r$ apply. Given n and ω_c, let $\mathcal{W}^n_{\omega_c}$ be given by Theorem 5.2. Further let*

$$F = \begin{bmatrix} 0 & I & 0 \\ 0 & 0 & I \\ 0 & 0 & \mathcal{S}_r \end{bmatrix}, \quad H = \begin{bmatrix} I & 0 & 0 \end{bmatrix}.$$

Suppose that given $\epsilon > 0$ $\exists$ $K \in \mathcal{R}^{9\times 3}$, $P \in \mathcal{R}^{(9+n)\times(9+n)}$, $P > 0$ such that the linear matrix inequalities

$$\left[\begin{array}{c|c} P\begin{bmatrix} F_i + KH & KC_W \\ 0 & A_W \end{bmatrix} + \begin{bmatrix} F_i + KH & KC_W \\ 0 & A_W \end{bmatrix}^T P + \begin{bmatrix} H^T \\ -C_W^T \end{bmatrix}\begin{bmatrix} H & -C_W \end{bmatrix} & P\begin{bmatrix} 0 \\ B_W \end{bmatrix} \\ \hline \begin{bmatrix} 0 & B_W^T \end{bmatrix} P & -\epsilon^2 I \end{array}\right] < 0,$$

$$F_i = \begin{bmatrix} 0 & I & 0 \\ 0 & 0 & I \\ 0 & 0 & \mathcal{S}(\boldsymbol{\omega}_r^i) \end{bmatrix}, \quad i = \{1, \ldots 8\} \tag{7.6}$$

are satisfied. Then, the constant gains

$$\begin{bmatrix} K_1 \\ K_2 \\ K_3 \end{bmatrix} := K$$

make the filter $\mathcal{F}$ internally stable. Furthermore, the operator $\mathcal{F}_p : \mathbf{p} \to \hat{\mathbf{p}}$ satisfies a low pass property with indices (ϵ, n) over $[0, \omega_c]$, that is, $||(\mathcal{F}_p - I)\mathrm{W}_{\omega_c}^n|| < \epsilon$.

The proofs of theorems 7.1 and 7.2 follow directly from the proofs of theorems 5.1 and 5.2 and can also be found in [14]. The robustness of the filter $\mathcal{F}$ with respect to uncertainties in the rotation matrix $R(t)$ can be analyzed using the steps outlined in Section 5. Similarly, the filter design procedure given in Section 6 applies to the design of filter 7.5.

8 Conclusions

This paper extended the theory of complementary filtering to the time-varying setting. In particular, the frequency domain interpretations of complementary filters were extended by resorting to the theory of linear differential inclusions and by converting the problem of weighted filter performance analysis into that of determining the feasibility of a related set of Linear Matrix Inequalities (LMIs). Using this set-up, it has been shown how the stability of the resulting filters as well as their "frequency-like" performance can be assessed using efficient numerical analysis tools that borrow from convex optimization techniques. The cases of complementing position information with that available from onboard Doppler sonar and accelerometers have been considered. The resulting design methodology was successfully applied to a design example. Future work will aim at extending these results to the discrete-time, multi-rate case.

References

[1] I. Bar-Itzhack and I. Ziv, "Frequency and time domain designs of strapdown vertical determination systems," *Proc. AIAA Guidance, Navigation and Control*, Williamsburgh, August 1986, pp. 505-515.

[2] G. Becker and A. Packard, "Robust performance of linear, parametrically varying systems using parametrically- dependent linear, dynamic feedback," *Systems and Control Letters*, 1993.

[3] S. Boyd, L. El Ghaoui, E. Feron and B. Balakrishnan. *Linear Matrix Inequalities in Systems and Control Theory.* SIAM Studies in Applied Mathematics, Philadelphia, 1994.

[4] K. Britting. *Inertial Navigation System Analysis.* Wiley-Interscience, 1971.

[5] R. Brockett. *Finite Dimension Linear Systems.* John Wiley and Sons, New Yorkm 1970 1992.

[6] R. Brown and P. Hwang. *Introduction to Random Signals and Applied Kalman Filtering.* Second Edition, John Wiley and Sons, Inc., 1992.

[7] R. Brown, "Integrated navigation systems and Kalman filtering: a perspective," *Journal of the Institute of Navigation*, Winter 1972-73, Vol. 19, N0.4, pp.355-362.

[8] Fryxell, D., P. Oliveira, A. Pascoal and C. Silvestre (1994). An integrated approach to the design and analysis of navigation, guidance and control systems for AUVs. *Proc. Symposium on Autonomous Underwater Vehicle Technology*, Cambridge, Massachusetts, USA.

[9] K. C. Goh, L. Turan, M. G. Safonov, G. P. Papavassilopoulos, and J. H. Ly, "Biaffine Matrix Inequlity Properties and Computational Methods," *Proc 1994 American Control Conference*, Baltimore, MD, 1994, pp. 850-855.

[10] G. Goodwin and M. Seron, "Fundamental design tradeoffs in filtering, prediction, and smoothing," *IEEE Trans. Automatic Control*, Vol. 42, N0.9, September 1997, pp.1240-1251.

[11] M. Green and D. Limebeer. *Linear Robust Control.* Prentice-Hall, 1995.

[12] K. Grigoriadis and J. Watson, "Reduced-order H_∞ and $L_2 - L_\infty$ filtering via linear matrix inequalities," *IEEE Trans. Aerosopace and Electronic Systems*, Vol. 33, N0.4, October 1997, pp. 1326-1338.

[13] D. Jourdan, "Doppler sonar navigation error propagation and correction" *Journal of the Institute of Navigation*, Vol. 32,No.1, Spring 1985, pp.29-56.

[14] I. Kaminer and A. M. Pascoal, "Navigation System Design Using Time-Varying Complementary Filters", Internal Report, Naval Postgraduate School, January 1998.

[15] M. Kayton and W. Fried (ed.). *Avionics Navigation Systems.* John Wiley and Sons, Inc., New York, 1969.

[16] C. Lin. *Modern Navigation, Guidance, and Control Processing.* Prentice-Hall, 1991.

[17] MatLab Application Toolbox, LMI Control. *The Math Works Inc.*,1997.

[18] S. Merhav. *Aerospace Sensor Systems and Applictions.* Springer-Verlag, 1996.

[19] K. Nagpal and P. Khargonekar, "Filtering and smoothing in an H_∞ setting," *IEEE Trans. Automatic Control*, Vol. 36, 1991, pp.152-166.

[20] C. Scherer, P. Gahinet and M. Chilali, "Multiobjective output-feedback control via LMI optimization," *IEEE Trans. Automatic Control*, Vol. 42, N0.7, July 1997, pp. 896-911.

[21] G. Siouris. *Aerospace Avionics Systems: a Modern Synthesis.* Academic Press Inc., 1993.

[22] J. Stambaugh and R. Thibault, "Navigation requirements for autonomous underwater vehicles," *Journal of the Institute of Navigation*, Vol. 39, No.1, Spring 1992, pp.79-92.

[23] M. Vidyasagar, *Control System Synthesis: a Factorization Approach,* MIT Press, 1985.

[24] J. Youngberg, "A novel method for extending GPS to underwater vehicles," *Journal of the Institute of Navigation*, Vol. 38, No.3, Fall 1991, pp.263-271.